

# Ferromagnetism in CePd<sub>1-x</sub>Rh<sub>x</sub> single crystals

S. HARTMANN<sup>a,\*</sup>, M. DEPPE<sup>a</sup>, N. OESCHLER<sup>a</sup>, N. CAROCA-CANALES<sup>a</sup>, J. SERENI<sup>b</sup>, C. GEIBEL<sup>a</sup>

<sup>a</sup>Max Planck Institute for Chemical Physics of Solids, Nothnitzer Str. 40, 01187 Dresden, Germany

<sup>b</sup>Laboratorio de Bajas Temperaturas, Centro Atomico Bariloche (CNEA), 8400 S. C. de Bariloche, Argentina

The orthorhombic CePd<sub>1-x</sub>Rh<sub>x</sub> alloy exhibits a continuous evolution from a ferromagnetic ground state at  $x = 0$  to intermediate-valence behavior for  $x = 1$ . Here, we report on specific heat  $C_p(T)$ , resistivity  $\rho(T)$  and magnetization  $M(T)$  measurements on single crystals in a Rh concentration range  $0.2 < x < 0.65$  exploring the ferromagnetic side of the magnetic phase diagram. The transport and thermodynamic properties of the ferromagnetic phase have been investigated in the temperature range from 300 K down to 0.35 K and analyzed in terms of a gap in the magnon spectrum and an underlying Kondo contribution. Crystal electric field parameters are deduced from specific heat measurements well above  $T_c$ . The competition between Kondo effect and ferromagnetism has been studied in dependence of the Rh concentration in the system. Particularly, the enhanced Sommerfeld coefficient  $\gamma(x)$  indicates strong Kondo interactions when the Curie temperature is reduced.

(Received April 1, 2008; accepted June 30, 2008)

**Keywords:** Ce compound, ferromagnetism, heavy fermion system

## 1. Introduction

The investigation of Ce-based intermetallic compounds with their large variety of unusual physical properties and phenomena has attracted attention for a long time. Especially, the study of the magnetism and the uncommon properties at very low temperatures related to the magnetic quantum critical points (QCP), where quantum fluctuations compete with classical thermal fluctuations, have been of great interest. There exists a large number of Ce-based antiferromagnets, that can easily be driven to a AFM-QCP by pressure or alloying. However, up to now a comparable example for an intermetallic Ce-compound exhibiting a FM-QCP has not been found yet. Theoretical predictions [1,2] for clean itinerant ferromagnets suggest that, by applying pressure, the ordering in these systems vanishes as a first order transition at finite temperatures. However, disorder introduced by alloying could smear this first order phase transition and lead to a continuous disappearance of the long-range magnetic order [3]. Thus, the appropriate modification of Ce ferromagnets upon doping may drive these systems close to a FM-QCP and offers the chance to study the emergence of ferromagnetic quantum critical behavior.

With the binary compound CePd<sub>1-x</sub>Rh<sub>x</sub> a good candidate was found to study the continuous suppression of FM ordering by means of alloying. The substitution of Pd by Rh leads to the decrease of the unit cell volume, and furthermore, to a change of the electronic surrounding of the Ce ion. The decrease of  $T_c$  to zero is traced over nearly two orders of magnitude until long-range FM order vanishes at a critical concentration of  $x_{crit}=0.87$ . Concomitantly to the suppression of the Curie temperature, the Kondo interactions are strongly enhanced

and finally the system enters an intermediate-valent regime. Whether the continuous disappearance of the FM order is caused by a smeared phase transition [4] or can be explained within the Griffiths phase scenario [5] is a matter of current discussion [6].

## 2. Experimental

The investigated samples of the CePd<sub>1-x</sub>Rh<sub>x</sub> doping series are new-generation single crystals with a higher residual resistivity ratio compared to the previously investigated poly crystals [6,7]. Samples in the concentration range  $0.2 < x < 0.9$  were grown in tantalum crucibles under Argon atmosphere using the Bridgman technique. With a pulling rate of 3-7 mm/h relatively large crystals exhibiting maximum sizes of  $m \approx 77$  mg were obtained. X-ray powder diffraction pattern confirm the orthorhombic CrB-structure throughout the whole doping range. Laue backscattering measurements indicate that the crystals grow as platelets perpendicular to the crystallographic  $b$ -axis. Additionally, electron microprobe analysis confirms the compositions to be very close to the starting ones with only a slight decrease of 2-3 % in the Pd/Rh ratio for samples with  $0.6 < x < 0.9$ , see also ref. [8]. Subsequent annealing of the specimens at 700 C for one week leads to a further improvement of sample quality evidenced by a slight reduction of the residual resistivity. However, no further effects of the annealing on the physical properties are observed.

The specific heat (heat pulse technique) and the resistivity (four-point ac set-up) measurements were carried out using a commercial PPMS (Quantum Design) with a <sup>3</sup>He refrigerator in the temperature range from 0.35 K to 300 K. Measurements of the DC magnetization were

performed with a commercial SQUID magnetometer (MPMS - Quantum Design) in the temperature range from 1.8 to 300 K.

### 3. Results

Here we report on the results of specific heat  $C_p(T)$ , resistivity  $\rho(T)$  and magnetization  $M(T)$  investigations with focus on the low Rh doping range  $x < 0.65$ , where the system clearly exhibits a ground state of long-range ferromagnetic order. The measurements performed on the new single crystals confirm the magnetic phase diagram deduced from polycrystal studies.

#### 3.1. Specific heat

Fig. 1 shows the magnetic contribution to the specific heat  $C_{mag}(T)$  in the doping series  $CePd_{1-x}Rh_x$  for  $x = 0.2, 0.4, 0.6$  and  $0.65$  single crystals in the temperature range  $0.35 \text{ K} < T < 10 \text{ K}$ . Single crystal  $C_p(T)$  data for higher Rh concentrations  $x = 0.7, 0.8$  and  $0.9$  have already been presented in [8]. The magnetic contribution was derived by subtracting the specific heat of the nonmagnetic reference compound LaRh from the total  $C_p$  of the magnetic systems  $C_{mag} = C_p - C_{LaRh}$ . The specific heat of LaRh is well-described by a sum of a  $T^3$  phononic term and a linear electronic contribution for  $T < 6 \text{ K}$ , with a Debye temperature of  $\sim 140 \text{ K}$  [9]. LaRh acts as a good phonon-reference to all investigated  $CePd_{1-x}Rh_x$  samples throughout the whole Rh doping range.

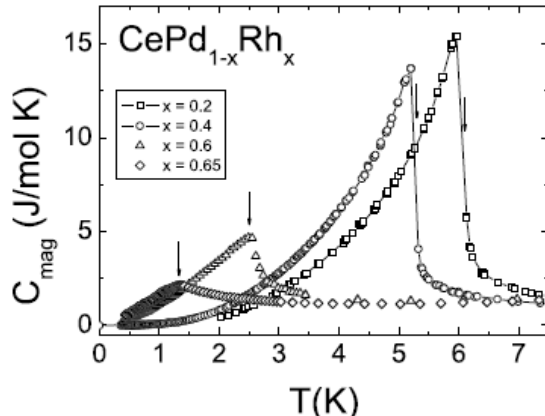


Fig. 1. Magnetic contribution to the specific heat  $C_{mag}(T)$  of  $CePd_{1-x}Rh_x$  arrows mark the ferromagnetic phase transitions.

The ferromagnetic phase transition appears as a sharp, lambda-shaped anomaly in  $C_{mag}(T)$  for  $x = 0.2$  and  $0.4$  with Curie temperatures of  $T_c = 6.1 \text{ K}$  and  $5.3 \text{ K}$ , respectively. These values are in agreement with the ones observed in the polycrystalline samples [6], however the anomalies are much sharper in the single crystals. With increasing Rh content the ferromagnetic ordering temperature is further suppressed to  $T_c = 2.5 \text{ K}$  for  $x = 0.6$

and to  $T_c = 1.33 \text{ K}$  in the  $x = 0.65$  sample. Besides the shifting of the FM transition temperature to lower  $T$  also the magnitude of the peak is reduced with increasing Rh content. Simultaneously, the anomaly broadens, but still the system exhibits a clearly ferromagnetic ground state. Low-T investigations on the polycrys-talline samples reveal the evolution of the ordering when increasing the Rh content to beyond 0.7 [6]. Previous measurements of the ac-susceptibility  $X_{ac}$  suggest, that the FM order is conserved until it vanishes at a critical concentration of  $x_{cri} = 0.57$ . However, a frequency dependence in  $x_{ac}$  becomes observable for  $x \approx 0.7$  and further increases with  $x$ , indicating a crossover to ferromagnetic cluster or spin glass behavior, which we attribute to a distribution of local Kondo energy scales due to the random Pd-Rh distribution. Also low temperature specific heat measurements in this doping range suggest the magnetic ordering being of short-range type [9].

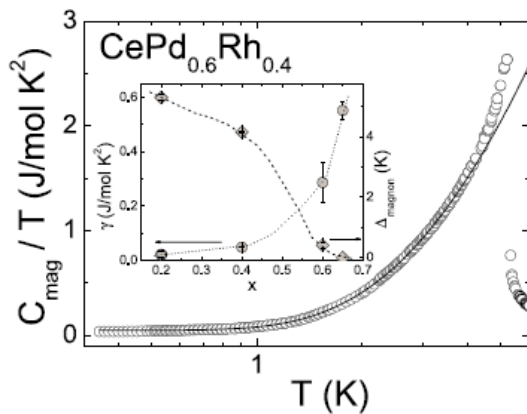


Fig. 2. Low temperature part of the magnetic specific heat  $C_{mag}/T$  for  $x = 0.4$ , solid line represents a fit to the data according to the given equation (see text). Inset: Sommerfeld coefficient  $\gamma$  and magnon gap  $\Delta$  derived from the above fit

Fig. 2 shows the low-temperature part of the magnetic specific heat divided by  $T$  for the  $x = 0.4$  sample. The temperature behavior of  $C_{mag}(T)$  in the FM phase well below  $T_c$  is described by an electronic and a magnonic contribution. The electronic contribution exhibits a linear temperature dependence, whereas the magnonic behavior is best described with a gap in the magnon excitation spectrum due to magnetic anisotropy. The data could be fitted according to the above considerations by  $C_{mag} = \gamma T + \beta T^{3/2} \exp(-\Delta/T)$ , yielding a moderate Sommerfeld coefficient  $\gamma = 50 \text{ mJ/mol K}^2$ ,  $\beta = 2 \text{ J/mol K}^{5/2}$  and a magnon gap  $\Delta = 4.2 \text{ K}$ , respectively. A similar analysis was performed for the Ce-based ferromagnet  $CeRu_2Ge_2$  exhibiting a Curie temperature of  $7.5 \text{ K}$  yielding similar values [10]. The inset of figure 2 shows the evolution of the Sommerfeld coefficient  $\gamma(x)$  and the magnon gap  $\Delta_{mag}(x)$  for the investigated samples as was derived from the above fit. With increasing Rh content the  $\gamma$  value obtained strongly increases up to a value of  $550 \text{ mJ/mol K}^2$  for  $x = 0.65$ , while the gap in the magnon

dispersion is continuously suppressed. The enhanced  $\gamma$  is the result of the increasing hybridization due to the replacement of Pd by Rh, that suppresses the local magnetism. The Sommerfeld coefficient reaches its highest value in the intermediate concentration range, where the Kondo interactions have overcome the ferromagnetic ones and dominate the behavior of the system. Low temperature specific heat measurements evidence a logarithmic divergence of  $C/T$  just below the critical concentration, evolving into a power law divergence above  $x_{crit}$ . With further increasing the hybridization strength, the system becomes intermediate-valent and  $\gamma$  is reduced again [9].

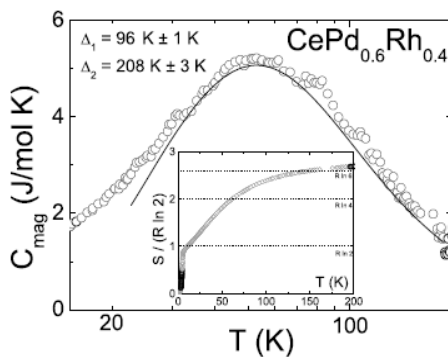


Fig. 3. High temperature part of magnetic specific heat  $C_{mag}$  for  $x=0.4$ ; solid line represents a Schottky fit to the data including two excited doublets. Inset: Magnetic entropy  $S_{mag}$  for  $x=0.4$ , dotted lines represent the entropy gain corresponding to the excitation of 1st, 2nd and 3rd crystal electric field level (doublets).

Considering the crystal electric field effects, the  $J=5/2$  multiplet ( $L=3$ ,  $S=1/2$ ) of the Ce<sup>3+</sup> ion in the orthorhombic environment splits into a ground state doublet and two excited doublets. Figure 3 shows the high temperature part of the magnetic specific heat, where the Schottky contribution due to these excited crystal electric field levels is observed as a broad anomaly ranging from 10 K to 200 K. The deduced magnetic entropy from  $C/T$  as shown in the inset of Fig. 3 indicates, that the full entropy  $S = R \ln 6$  for the three doublets of the Ce<sup>3+</sup> ion is reached at 200 K. This implies both excited CEF levels contributing to the observed anomaly. From a Schottky fit to the data, assuming two excited doublets, the energy separations  $\Delta_1$  and  $\Delta_2$  from the ground state were extracted. According to the fit the two excited levels in  $x = 0.4$  are at  $\Delta_1 = 96$  K and  $\Delta_2 = 208$  K. For the  $x = 0.7$  polycrystalline sample, the position of the first excited level was estimated from dc-susceptibility, using a very simplified expression applicable in the low-temperature range ( $T < ACEF$ ). From this fit a  $\Delta_1 = 70$  K was obtained [6]. This value corresponds to the value estimated from specific heat for the  $x = 0.4$  sample.

### 3.2. Electrical resistivity

In Fig. 4 the electrical resistivity normalized to its

room temperature value  $\rho(T)/\rho_{300K}$ , is plotted on a logarithmic scale for  $0.2 < x < 0.65$ . The electrical resistivity  $\rho(T)$  shows metallic behavior as it decreases continuously for  $x = 0.2$  and 0.4. At the FM phase transition a sharp drop appears due to freezing of spin-disorder scattering in the ordered state. The drop shifts to lower temperatures upon increasing  $x$  and becomes less pronounced. The Curie temperatures derived from resistivity data are in agreement with specific heat results. A strong increase of the residual resistivity  $\rho_o$  with increasing  $x$  is obvious, evidencing the increasing disorder in the system. The maximum value of  $\rho_o$ , however, occurs at  $x = 0.65$ , while maximum alloying disorder is expected at  $x = 0.5$ . With further increasing the Rh content to beyond  $x = 0.7$ , the residual resistivity decreases again. For Rh concentrations  $x < 0.5$  the decrease of the resistivity is followed by a logarithmic increase in the temperature range  $5 K < T < 10 K$  just above  $T_c$ , before the drop indicates the system is entering the magnetic phase. This increase is due to the presence of Kondo interactions becoming stronger with increasing Rh content. A further discussion of the interplay between ferromagnetic ordering and Kondo interactions will be given elsewhere.

In analogy to the specific heat data at low  $T$ , the temperature behavior of the magnetic resistivity  $\rho_{mag}$  within the magnetic phase was analyzed considering a spin-wave contribution with a gap in the magnon spectrum. The data well below  $T_c$  was fitted according to  $\rho(T) = \rho_0 + AT^2 + aT\Delta(1 + 2T/\Delta) \exp(-\Delta/T)$  [11], whereas  $AT^2$  accounts for Fermi-liquid quasiparticle excitations. For  $x = 0.2$  and 0.4 the fitting yields values for  $A_{mag}$  in the same order of magnitude as found from the specific heat analysis. For  $x > 0.6$  the scattering of electrons by spin waves is negligible and the data below  $T_c$  is well described by a  $T^2$ -behavior. This is consistent with the results from the specific heat (inset of figure 2), where the magnon gap closes with increasing  $x$  and the magnonic contribution decreases.

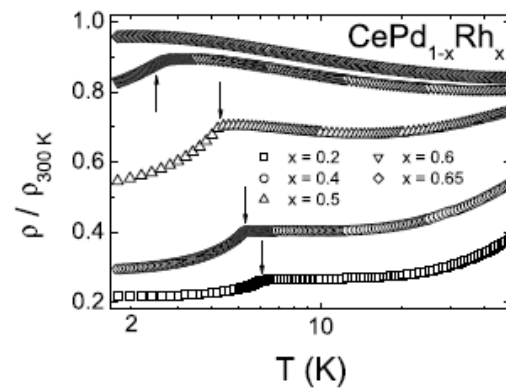


Fig. 4. Electrical resistivity  $\rho(T)$  vs.  $T$  of  $CePd_{1-x}Rh_x$  for  $0.2 < x < 0.65$  with the current perpendicular to the  $b$ -direction, arrows mark the Curie temperatures,  $x = 0.5$  sample is polycrystalline (data by P. Pedrazzini, unpublished). Dashed lines represent the logarithmic temperature behavior above

### 3.3. Magnetization

Fig. 5 presents the temperature dependence of the magnetization  $M(T)$  for the  $x = 0.2$  and  $0.4$  sample in a small external field of  $1.8$  mT along the crystallographic c-direction. Measurements were performed in the temperature range  $2$  K  $< T < 10$  K. The measurements display the typical behavior for a ferromagnetic compound, exhibiting a sharp increase of the magnetization at  $T_c$  and a saturation of the magnetization below  $T_c$ . The value of  $T_c$  is obtained from the inflection point of the  $M(T)$ -curve, determined by the minimum in the derivative. The extracted values of  $T_c = 6.1$  K and  $5.3$  K for  $x = 0.2$  and  $0.4$ , respectively, correspond to the ones observed in specific heat and resistivity measurements.

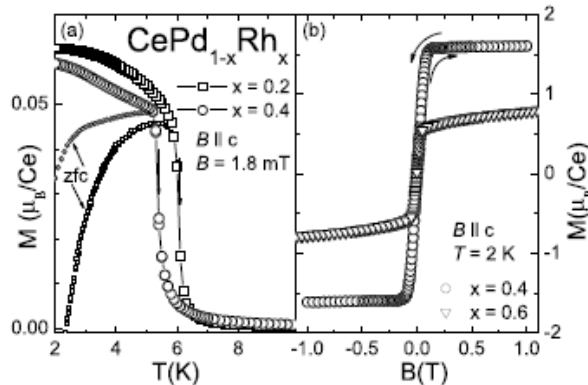


Fig. 5. (a) Magnetization  $M$  vs.  $T$  of  $\text{CePd}_{1-x}\text{Rh}_x$  for  $x = 0.2$  and  $0.4$  along  $c$ -direction in external field of  $1.8$  mT, arrows mark the Curie temperatures derived from the inflection point of the curves, (b) Field dependence of the magnetization  $M$  of  $\text{CePd}_{1-x}\text{Rh}_x$  for  $x = 0.4$  and  $0.6$  at  $2$  K with the external field along the  $c$ -axis.

Measurements of the field dependence of the magnetization for  $x = 0.4$  and  $0.6$  in the ferromagnetic regime well below  $T_c$  are shown in Fig. 5. At  $2$  K the magnetization reaches the saturation moment of  $1.6 \mu/\text{Ce}$  at an external field of  $\pm 0.5$  T in the  $x = 0.4$  sample along the crystallographic  $c$ -direction. The magnitude of the observed moment implies a significant contribution of the  $|\pm 5/2\rangle$  wave function to the CEF ground state doublet. In the  $x = 0.6$  sample a further reduction of the saturation magnetization to  $1 \mu/\text{Ce}$  at a field of  $5$  T along the  $c$ -direction is observed. This further reduction of the moment with increasing  $x$  is likely an indication of screening of moments due to growing Kondo interactions in the system. No hysteresis effects were observed for the investigated concentrations  $x = 0.4$  and  $0.6$  within the limit of the experimental resolution.

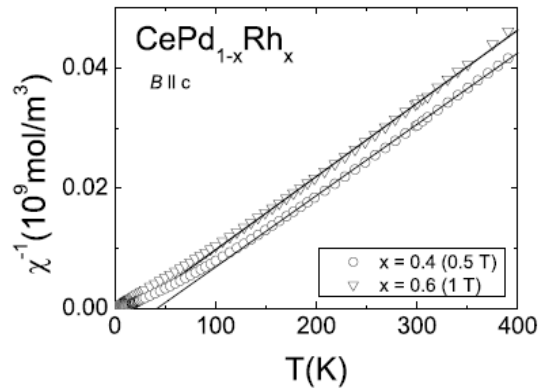


Fig. 6. Inverse magnetic susceptibility  $\chi^{-1}$  vs.  $T$  of  $\text{CePd}_{1-x}\text{Rh}_x$  for  $x = 0.4$  and  $0.6$ , solid lines represent the Curie-Weiss fit to the data. Effective moment and paramagnetic Curie temperature derived from the fit are given in the text.

In the high temperature limit the magnetic susceptibility with the magnetic field along the  $c$ -direction follows a Curie-Weiss behavior as evidenced from figure 6, where  $1/\chi$  is plotted as a function of temperature. The effective moments in the paramagnetic state derived from the slope of the curves are  $2.32 \mu_B$  and  $2.29 \mu_B$  for  $x = 0.4$  and  $0.6$ , respectively. These values are quite close to the expected moment of  $2.54 \mu_B$  for the  $^2\text{F}_{5/2}$  ground state of the free  $\text{Ce}^{3+}$  ion. The paramagnetic Curie temperature  $T_c$  was estimated to  $42$  K in the  $x = 0.4$  sample and  $20$  K in  $x = 0.6$  indicating a dominant ferromagnetic exchange. Below  $80$  K the susceptibility starts to deviate from a Curie-Weiss behavior, likely because of crystal electric field effects.

### 4. Discussion

The thermodynamic and transport properties of  $\text{CePd}_{1-x}\text{Rh}_x$  single crystals reveal a true long-range ordered ferromagnetic ground state for  $x < 0.6$  and confirm the magnetic phase diagram that was established for the polycrystalline samples [6]. However, the increased quality is evident by the sharper anomaly in the specific heat at  $T_c$  and the lower residual resistivity. The long-range ferromagnetic type of ordering below the Curie temperature for  $x < 0.6$  has been confirmed by magnetization measurements in a small applied magnetic field.  $M(B)$  reveals a step-like increase at  $T_c$  due to the spontaneous magnetization of the ferromagnetic ground state and a slightly increasing magnetization below  $T_c$ . Furthermore, the electrical resistivity exhibits a sharp drop when the system enters the ferromagnetic phase, as spin-disorder scattering is significantly reduced.

The behavior of the  $\text{CePd}_{1-x}\text{Rh}_x$  single crystals is governed by the competition between Kondo screening and RKKY interactions, also taking CEF effects into account. The investigated properties evidence the

continuous suppression of the ferromagnetic ordering temperature upon increasing the Rh content. At the same time the Kondo energy scale is strongly enhanced. The anomaly in  $C_{mag}$  indicating the phase transition shifts to lower temperatures with increasing  $x$ . For  $x > 0.6$  the anomaly significantly broadens and becomes less pronounced due to the increasing structural and magnetic disorder in the Ce environment. The drop in the electrical resistivity indicating the onset of FM ordering also shifts to lower temperatures, while the feature is washed out. As  $T_c$  decreases the ordered moment as it is measured by magnetization decreases as well. The magnetic entropy reaches 80 % of  $R \ln 2$  at  $T_c$  in the  $x = 0.4$  sample, this value is further decreased to around 50 % in  $x = 0.65$ , as already reported in reference [12]. Entropy is shifted to higher temperatures, indicating increasing hybridization of the Ce 4f electrons with the conduction electrons, Kondo interactions cause a reduction of ordered Ce moment. The full entropy gain of  $S = R \ln 2$  is not reached below 10 K.

With increasing Rh content the residual resistivity is enhanced. It shows maximum values at  $x \ll 0.65$ , which is contrary to the evolution of  $\rho_0$  that is only due to atomic disorder introduced by the alloying. Here, the residual resistivity is expected to peak at  $x \ll 0.5$ . The further enhancement of  $\rho_0$  beyond  $x = 0.5$  suggests that additional magnetic contributions to the scattering mechanisms are present at intermediate Rh concentrations, shifting the maximum in the residual resistivity to higher  $x$ . Furthermore, the observed increase in  $\rho(T)$  below 10 K for  $x > 0.5$  in the presence of a clear ferromagnetic ground state points to the coexistence of ferromagnetism and Kondo interactions in the intermediate concentration range.

A further analysis of the low-temperature specific heat and resistivity yields the nature of the magnetic phase. A fit to  $C_{mag}$  well below  $T_c$  shows that apart from the enhanced electronic contribution the low temperature specific heat is due to a ferromagnetic magnon spectrum with an anisotropy gap. The gap is found to be of the order of the Curie temperature and closes with increasing  $x$ . The same result is derived from a fit to the magnetic resistivity, which can be well described by contributions due to heavy quasiparticle scattering and due to scattering of electrons by spin waves. Furthermore, the analysis of the specific heat shows the strong increase of the Sommerfeld coefficient with  $x$  in the investigated concentration range. This directly evidences the growing importance of Kondo interactions in CePd<sub>1-x</sub>Rh<sub>x</sub> with increasing  $x$ .

## 5. Conclusion

A series of new single crystals were prepared on the doping series CePd<sub>1-x</sub>Rh<sub>x</sub>. Magnetization, specific heat and resistivity measurements were carried out to investigate the ferromagnetic ordering in different single-crystalline samples with  $0.2 < x < 0.65$ . Our investigations confirm the behavior found in the previously investigated polycrystalline specimens. With increasing Rh content the hybridization is enhanced, leading to a continuous

suppression of the long-range ferromagnetic ordering and a strong increase of the Kondo energy scale. Our results show, that these mechanisms are the same in poly- and single-crystalline specimens. The low-temperature part of the magnetic specific heat anomaly was fitted by an electronic and a magnonic contribution with an anisotropy gap in the magnon spectrum. From high-temperature specific heat data the positions of the excited CEF doublets were obtained for  $x = 0.4$  being 96 K and 208 K, respectively. Resistivity shows a sharp drop at the ferromagnetic ordering temperature, the low  $T$  behavior was fitted including a magnon scattering term yielding the same gap as found in specific heat. A logarithmic upturn in  $\rho(T)$  indicates the presence of Kondo interactions above  $x = 0.6$ . Magnetization measurements reveal a suppression of the saturation moment in the ferromagnetic state with increasing Rh content in accordance to the enhancement of Kondo interactions.

## Acknowledgements

The authors would like to acknowledge financial support from COST P-16 action.

## References

- [1] D. Belitz et T. R. Kirkpatrick, Thomas Vojta, Phys. Rev. Lett. **82**, 4707 (1999).
- [2] T. R. Kirkpatrick, D. Belitz, Phys. Rev. B **67**, 024419 (2003).
- [3] T. Vojta, Phys. Rev. Lett. **90**, 107202 (2003).
- [4] R. Sknepnek, T. Vojta, Phys. Rev. B **69**, 174410 (2004).
- [5] R. B. Griffiths, Phys. Rev. Lett. **23**, 17 (1969).
- [6] J. G. Sereni et al., Phys. Rev. B **136**, 024432 (2005).
- [7] J. G. Sereni, R. Küchler, C. Geibel [http://www.sciencedirect.com/science?\\_ob=Article\\_URL&\\_udi=B6TVH-4FG4VC5-1&\\_user=2795744&\\_rdoc=1&\\_fmt=&\\_orig=search&\\_sort=d&view=c&\\_acct=C000058829&\\_version=1&\\_urlVersion=0&\\_userid=2795744&md5=d1fc2ba21def0f9efb676708cd3347a2-aff2](http://www.sciencedirect.com/science?_ob=Article_URL&_udi=B6TVH-4FG4VC5-1&_user=2795744&_rdoc=1&_fmt=&_orig=search&_sort=d&view=c&_acct=C000058829&_version=1&_urlVersion=0&_userid=2795744&md5=d1fc2ba21def0f9efb676708cd3347a2-aff2), Physica B **359-361** (2005) 41.
- [8] M. Deppe, P. Pedrazzini, N. Caroca-Canales, C. Geibel, J.G. Sereni et al., Physica B **378-380**, 96 (2006).
- [9] A P Pikul, N Caroca-Canales, M Deppe, P Gegenwart, J G Sereni, C Geibel, F Steglich., J. Phys.: Condens. Matter **18**, L535 (2006).
- [10] A. Bohm et al., J. Magn. Magn. Mater. **76-77**, 150 (1988).
- [11] N. H. Andersen, H. Smith, Phys. Rev. B **19**, 355 (1979).
- [12] J. P. Kappler et al., Physica B **171**, 346 (1991).
- [13] J. G. Sereni et al., Physica B **215**, 273 (1995).

<sup>\*</sup>Corresponding author. [hartmann@cpfs.mpg.de](mailto:hartmann@cpfs.mpg.de)